MINERALOGICAL MAGAZINE, JUNE 1984, VOL. 48, PP. 243–9

Occurrence of some Ni- and Sn-rich minerals in copper converter slags

E. WEARING*

Department of Geology and Mineralogy, Oxford University, Parks Road, Oxford OX1 3PR

ABSTRACT. The chemistry of opaque spinel, delafossite ($Cu_2O \cdot Fe_2O_3$), cuprite (Cu_2O), cassiterite, nickel-olivine (Ni_2SiO_4), and bunsenite (NiO) from some copper converter slags has been investigated by electron microprobe analysis. The spinel has a complex composition containing up to 33.89% NiO and 47.69% SnO_2, ranging from essentially Ni_2SnO_4 to $(Ni,Fe^{2+})Fe_2^{3+}O_4$. The associated delafossite contains up to 19.18% NiO and 38.15% SnO_2. The chemical variation of the mineral phases is evaluated, and it appears that Ni^{2+} enters the spinel and delafossite to charge-balance the octahedrally coordinated Sn^{4+}.

THIS paper describes the mineralogy of some slowly cooled copper converter slags, which had been cast into approximately hemispherical ladles 1 m in diameter and allowed to air-cool. From the large number of samples collected, three main mineral assemblages have been recognized:

1. nickel-olivine (Ni_2SiO_4) + spinel + delafossite ($Cu_2O \cdot Fe_2O_3$) + cuprite (Cu_2O) + cassiterite + bunsenite (NiO)
2. cassiterite + spinel + delafossite + cuprite
3. spinel + delafossite + cuprite.

All samples contain yellow to orange-yellow coloured glass, which represents rapidly cooled residual liquid, and shows no evidence of devitrification. Fifteen specimens, chosen as representative samples, have been studied to investigate the petrography and crystal chemistry of these converter slags, which have essentially SnO_2–NiO–ZnO–Cu_2O–PbO–Fe-oxide–SiO_2 bulk compositions.

Analytical techniques. The compositions of the phases were determined by extensive electron microprobe analysis using a C.S.I. Microscan 9 instrument. Computer corrections for ZAF effects were applied to all raw data. Spectrometer scans were used to detect the constituent elements for each phase. Electron microprobe analysis is occasionally complicated by interferences between elements. These can often be overcome by choosing analytical lines that avoid interference, or if this is impossible, by applying interference corrections. Empirical corrections were calculated for interferences at the Ca-$K\alpha$, Mg-$K\alpha$, Al-$K\alpha$, Si-$K\alpha$, and Na-$K\alpha$ lines.

* Present address: 210 Wingrove Road, Newcastle upon Tyne NE4 9DD.

Petrography

Accurate modal percentages of the different mineral phases were determined by point-counting (12 points/mm), and are presented in Table I. Significant amounts of metallic copper have been physically entrained in the slag. It tends to form as globular bodies up to 2.50 mm in diameter, dispersed throughout the slag. The spinel and cassiterite often include fine, globular metallic copper particles, indicating that the copper was probably initially finely disseminated throughout the molten slag. Under reflected light the large, globular metallic copper bodies have irregular outlines (fig. 1) and are surrounded by pear-shaped droplets of metallic copper which are coalescing with the main globule.

Nickel-olivine is lime-green in colour. In sample BCMB(BB)-2064 it forms a euhedral phenocryst phase (up to 1.40 × 0.33 mm in size), which is set in a groundmass formed by the other minerals. These nickel-olivine crystals have numerous glass inclusions, which suggest a fast growth rate. Towards the rim of these crystals, mineral inclusions appear in the order spinel, delafossite, and cuprite.

In samples CW-19, 26, and 31 the shape of the nickel-olivine crystals has been corroded as a result of apparent resorption by the liquid. Those crystals retaining their original shape have no mineral inclusions, except for the penetration of delafossite laths into the outer rims.

Cassiterite forms as colourless, high-relief needles up to 0.60 mm long and 0.05 mm square in cross-section. It forms relatively large crystals in assemblage 2 samples, and probably crystallizes before the spinel.

Table I. Modal percentages of the mineral phases in the selected copper converter slags (tr. = trace)

	Assemblage 1				Assemblage 2						Assemblage 3				
	BB-2064	CW-19	CW-26	CW-31	CW-1	CW-2	CW-5	CW-23	CW-33	CW-34	CW-4	CW-8	CW-20	CW-21	CW-29
spinel	4.2	35.6	8.8	30.8	40.4	39.8	46.3	54.6	32.1	43.7	44.7	13.6	15.9	29.6	47.8
cassiterite	5.1	4.2	-	9.4	14.3	14.6	9.1	13.3	11.3	10.8	-	-	-	-	-
cuprite	20.2	10.2	36.4	15.5	15.8	16.3	21.1	8.0	23.6	24.4	31.5	29.6	26.3	13.8	16.7
delafossite	20.0	9.8	23.3	-	-	-	11.6	-	8.2	-	17.3	21.8	23.9	18.1	24.2
nickel-olivine	40.4	35.2	19.8	20.2	-	-	-	-	-	-	-	-	-	-	-
bunsenite	2.0	tr.	1.6	tr.	-	-	-	-	-	-	-	-	-	-	-
glass	8.1	5.0	10.1	24.1	29.5	29.3	11.9	24.1	24.8	21.1	7.5	35.0	33.9	38.5	11.3

(Because of the relatively fine grain size, 3,000 points were considered necessary to achieve a statistically-representative sample of the phases.)

In assemblage 1 samples there is a lack of textural evidence for the position of cassiterite in the crystallization sequence. However, its small size and lack of textural relations with other minerals suggests that cassiterite is a late-stage mineral.

Spinel is opaque and has an octahedral to sub-octahedral habit, and is present in nearly all samples. Its size varies between and within samples, although three ranges have been recognized: (i) large-sized spinel up to 0.40 mm across, restricted to certain samples (independent of assemblage), (ii) medium-sized spinel up to 0.21 mm across, and (iii) small-sized spinel up to 0.10 mm across; the latter two types are present in all spinel-bearing samples.

The large-sized spinel crystals have glass inclusions, which are probably a result of a fast growth rate. In comparison, the medium- and small-sized spinels are inclusion-free which, combined with the size differences, suggests that there may have been two periods of spinel crystallization. If so, the large-sized spinels would have crystallized first.

Delafossite is lath-shaped (up to 9.20 × 0.10 mm, sample CW-20) and opaque. In assemblage 3 samples the delafossite laths often terminate abruptly against spinel octahedra which suggests that the latter crystallized first.

Cuprite forms with a polygonal shape (up to 0.05 mm across), showing brilliant red internal reflections. It appears to be the final crystalline phase in all samples since it tends (*a*) to surround the other phases (fig. 2) and (*b*) to be spread throughout the glass. In many samples cuprite is included in the outer rims of the delafossite, indicating that the general crystallization sequence is spinel, delafossite, and cuprite.

Bunsenite crystallizes as an accessory mineral and shows no relationship with the other phases.

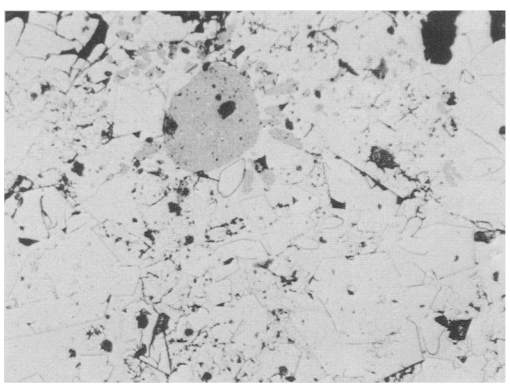

FIGS. 1 and 2. FIG. 1 (*left*). Photomicrograph showing (top centre) the irregular outline of metallic copper (dark) globules and the surrounding pear-shaped droplets of metallic copper. Other phases (light) are spinel (octahedral outline), cuprite (small, polygonal masses), and interstitial glass. Reflected light (sample CW-8); field of view is 0.75 mm across. FIG. 2 (*right*). Cuprite (dark, globular mineral) set in glass (light), surrounding spinel octahedra and delafossite laths. Plane polars (sample CW-7); field of view is 3.00 mm across.

The order of crystallization for the three assemblages can be established from these petrographic relationships:

assemblage 1 nickel-olivine, spinel, delafossite, cuprite/cassiterite/bunsenite
assemblage 2 cassiterite, spinel, (delafossite), cuprite
assemblage 3 spinel, delafossite, cuprite.

Chemical variation of the phases

The resorption of the nickel-olivine by the liquid (now represented by glass) has been investigated using the electron microprobe. However, step-scanning failed to detect any chemical gradients, as might be expected for resorption. The resolution of the electron microprobe at a boundary is 0.004 mm from the boundary, and so if any resorption was taking place close to (or at) the boundary it would be beyond detection.

The varied mineralogy of these slags suggests a variability in their chemistry. A selection of analyses will be presented, chosen to be representative chemically of the mineral phases studied. Since the total iron content of an electron microprobe analysis is expressed as FeO, any mineral with an appreciable Fe_2O_3 content would be recognized by a large deviation from the stoichiometric formula: only spinel has a large excess in the number of cations present in its formula. The Fe_2O_3 concentrations in the spinel analyses were estimated by reallocating oxygens to give a total of 3 cations, and then solving for Fe^{3+} and Fe^{2+}.

Spinel. Representative analyses of spinel are presented in Table II. No significant chemical variation can be found between the three sizes of spinel, although spinel composition varies between assemblages.

The SiO_2, TiO_2, and CaO contents of the spinels are of minor importance. Al_2O_3 and MgO are not significant in comparison to the other oxides, and their variation is probably a result of their concentrations in the liquid.

The major oxides are Fe_2O_3 (2.20–62.78 wt. %), SnO_2 (1.93–47.69 wt. %), NiO (10.94–33.89 wt. %), ZnO (2.25–20.02 wt. %), and FeO (2.79–12.48 wt. %). In some samples the spinel is in contact with cassiterite, and so (for equilibrium) the SnO_2 content must be a maximum value of ionic replacement in the spinel structure. Although the spinel is in contact with cuprite (Cu_2O), the spinel structure requires the Cu content to be treated as CuO (0.76–2.96 wt. %).

Delafossite. Electron microprobe analyses of representative delafossites are presented in Table III. The total iron content is expressed as Fe_2O_3 and total copper content as Cu_2O, to satisfy the formula $Cu_2O \cdot Fe_2O_3$ and the cation total is close to stoichiometry. These delafossites contain significant amounts of SnO_2 (up to 38.15 wt. %) and NiO (up to 19.18 wt. %).

Cassiterite. There is no substitution of other elements into the cassiterite structure.

Cuprite. There is limited substitution of FeO (up to 0.23 wt. %) and NiO (up to 0.10 wt. %) into the cuprite structure.

Bunsenite (Table IV) has up to 2.62 wt. % ZnO (BB-2064), 2.26 wt. % CuO (CW-35), 4.53 wt. % FeO (BB-2064), and 0.46 wt. % MgO (CW-35).

Nickel-olivine. The core and rim compositions of nickel-olivine from BB-2064 are given in Table IV. Nickel-olivine has up to 1.12 wt. % CuO, and shows some zoning. Towards the rim there appears to be a substitution of $Zn^{2+} + Fe^{2+}$ for $Ni^{2+} + Mg^{2+}$, at approximately constant Cu^{2+}.

Glass. These are essentially lead-silicate glasses, with varying amounts of all other oxides although these have been largely depleted from the original liquid. The lead-silicate composition would be expected eventually to crystallize a lead-silicate mineral. There is no evidence in these slags to support this hypothesis. It seems possible that the lead-silicate glass is easy to supercool since there is no sign of devitrification: lead is sometimes used in the glass-making process to prevent devitrification. The system PbO–SiO_2 has been found to crystallize Pb_2SiO_4 whatever the composition (Ott and McLaren, 1970). Lead slags crystallize Pb_2SiO_4 (Edwards, 1949), which indicates that its formation is not restricted to the experimental system.

Chemical variation of the mineral phases

This paper provides new chemical data for spinel, delafossite, and nickel-olivine, and an evaluation of their chemical variation may be of interest to mineralogists. Unfortunately, there are few other data on similar slags with which to compare these analyses.

Spinel

Only the spinels of assemblages 2 and 3 are suitable for an evaluation of chemical variation; those of assemblage 1 are best described as spinels rich in NiO and SnO_2, with significant concentrations of Fe_2O_3, FeO, and ZnO.

Fe_2O_3/SnO_2. Inspection of molecular proportions shows that the spinel analyses in Table II do not maintain structural balance of $R^{3+}:R^{2+} = 2:1$, due to the molecular proportions of divalent and trivalent cations. Butler (1978) described SnO_2-rich magnetite from a tin reverberatory slag, and proposed that Sn^{4+} is only able to substitute for

Table II. Representative electron microprobe analyses of the spinel phase

	Assemblage 1			Assemblage 2				Assemblage 3			
	CW19B	CW19G	CW31A	CW1D	CW5F	CW23F	CW33B	CW8D	CW29A	CW29B	CW30A
SiO_2	0.31	0.34	0.45	0.00	0.28	0.38	0.22	0.10	0.21	0.22	0.29
Al_2O_3	0.47	0.56	0.57	0.70	1.61	0.06	0.43	0.94	5.55	8.09	0.60
TiO_2	0.07	0.03	0.20	0.06	0.07	0.03	0.10	0.05	0.14	0.30	0.05
Fe_2O_3	18.53	6.37	25.67	7.20	46.45	2.20	50.15	62.78	52.38	56.19	12.28
FeO	5.62	10.87	5.64	3.17	7.81	8.52	7.66	7.62	12.48	11.30	7.33
MgO	0.33	0.45	0.47	0.71	0.79	0.42	0.27	0.57	2.73	2.62	0.56
MnO	0.00	0.00	0.00	0.02	0.00	0.00	0.00	0.10	0.00	0.00	0.00
CaO	0.19	0.23	0.18	0.00	0.09	0.25	0.09	0.00	0.06	0.01	0.24
Cr_2O_3	0.19	0.19	0.00	0.00	0.00	0.38	0.00	0.00	0.32	0.47	0.00
SnO_2	34.78	44.30	28.18	43.33	13.74	47.69	12.44	2.28	7.48	1.93	37.96
CuO	0.97	1.20	1.39	1.18	1.51	1.49	1.09	1.67	2.96	1.53	0.74
NiO	33.89	31.11	22.99	22.81	23.64	31.08	16.80	16.09	10.94	13.35	25.19
ZnO	3.25	3.95	11.54	20.02	2.83	7.73	11.37	6.41	5.55	4.43	10.64
PbO	0.00	0.00	0.00	0.07	0.00	0.00	0.00	0.09	0.00	0.00	0.00
	98.60	99.60	97.28	99.27	98.81	100.23	100.61	98.70	100.80	100.44	95.88
STRUCTURAL FORMULA BASED ON 4 OXYGENS											
Si	0.014	0.016	0.021	0.000	0.012	0.019	0.009	0.004	0.008	0.008	0.014
Al	0.026	0.032	0.031	0.040	0.078	0.003	0.021	0.044	0.248	0.349	0.035
Ti	0.002	0.001	0.007	0.002	0.002	0.001	0.003	0.001	0.004	0.008	0.002
Cr	0.007	0.007	0.000	0.000	0.000	0.015	0.000	0.000	0.010	0.014	0.000
Fe3+	0.647	0.230	0.885	0.265	1.442	0.081	1.548	1.873	1.493	1.548	0.452
Sn	0.643	0.848	0.515	0.845	0.226	0.931	0.203	0.036	0.113	0.028	0.741
	1.339	1.134	1.459	1.152	1.760	1.050	1.784	1.958	1.876	1.955	1.244
Fe2+	0.218	0.437	0.216	0.130	0.269	0.349	0.263	0.253	0.395	0.346	0.300
Mg	0.023	0.032	0.032	0.052	0.049	0.031	0.017	0.034	0.154	0.143	0.041
Mn	0.000	0.000	0.000	0.001	0.000	0.000	0.000	0.003	0.000	0.000	0.000
Ca	0.009	0.012	0.009	0.000	0.004	0.013	0.004	0.000	0.002	0.000	0.013
Cu	0.034	0.044	0.048	0.044	0.047	0.055	0.034	0.050	0.085	0.042	0.027
Ni	1.264	1.201	0.847	0.897	0.784	1.223	0.554	0.513	0.333	0.393	0.991
Zn	0.111	0.140	0.390	0.723	0.086	0.279	0.344	0.188	0.155	0.120	0.384
Pb	0.000	0.000	0.000	0.001	0.000	0.000	0.000	0.001	0.000	0.000	0.000
	1.661	1.866	1.541	1.848	1.240	1.950	1.216	1.042	1.124	1.045	1.755

Table III. Representative electron microprobe analyses of the delafossite

	Assemblage 1		Assemblage 3				
	CW19I	CW26B	CW4C	CW8N	CW20E	CW21J	CW29K
SiO_2	0.19	0.19	0.15	0.11	0.04	0.29	0.08
Al_2O_3	0.40	0.34	0.41	0.45	1.99	1.12	0.90
TiO_2	0.03	0.03	0.10	0.13	1.25	0.51	0.27
Fe_2O_3	4.10	1.96	19.49	34.24	40.20	37.66	38.89
MgO	0.21	0.28	0.42	0.36	0.51	0.54	0.86
CaO	0.20	0.23	0.16	0.08	0.06	0.08	0.09
MnO	0.00	0.00	0.00	0.00	0.00	0.00	0.00
SnO_2	36.91	38.15	26.01	13.42	7.12	10.43	12.08
Cu_2O	40.04	39.97	42.02	44.63	46.48	45.18	45.41
NiO	17.85	19.18	10.48	5.35	2.57	3.62	1.92
ZnO	0.00	0.06	0.00	0.28	0.01	0.00	0.31
	99.93	100.39	99.24	99.05	100.23	99.43	100.81
STRUCTURAL FORMULA BASED ON 2 OXYGENS							
Si	0.006	0.006	0.004	0.003	0.001	0.008	0.002
Al	0.014	0.012	0.014	0.014	0.059	0.034	0.027
Ti	0.001	0.001	0.002	0.003	0.024	0.010	0.005
Fe3+	0.092	0.044	0.414	0.692	0.766	0.737	0.751
Mg	0.009	0.013	0.018	0.014	0.019	0.021	0.033
Ca	0.006	0.007	0.005	0.002	0.002	0.002	0.002
Mn	0.000	0.000	0.000	0.000	0.000	0.000	0.000
Sn	0.440	0.457	0.293	0.144	0.072	0.108	0.124
Ni	0.429	0.463	0.238	0.116	0.052	0.076	0.040
Zn	0.000	0.001	0.000	0.006	0.000	0.000	0.006
	0.997	1.004	0.991	0.994	0.995	0.996	0.990
Cu+	1.005	1.008	0.997	1.007	0.989	0.987	0.979
	1.005	1.008	0.997	1.007	0.989	0.987	0.979

(The delafossite crystals of CW-5 and CW-33, which are both assemblage 2 samples, were too small for electron microprobe analysis.)

Table IV. Representative electron microprobe analyses of the bunsenite and nickel-olivine

	BUNSENITE			NICKEL-OLIVINE (BB-2064)	
	BB-2064	CW-26	CW-35	core	rim
SiO_2	0.00	0.00	0.00	29.17	29.32
Al_2O_3	0.24	0.11	0.17	0.09	0.06
TiO_2	0.00	0.00	0.00	0.02	0.03
FeO	4.53	3.75	1.74	7.26	2.28
MgO	0.23	0.42	0.46	0.77	0.17
CaO	0.00	0.03	0.03	0.04	0.04
MnO	0.00	0.00	0.00	0.10	0.11
SnO_2	0.46	0.23	0.16	0.08	0.07
CuO	1.68	1.83	2.26	0.82	1.12
NiO	89.65	93.02	94.39	63.94	61.39
ZnO	2.62	0.69	0.00	3.55	5.37
	99.41	100.08	99.21	99.84	99.96
STRUCTURAL FORMULA BASED ON :-					
	10 OXYGENS			16 OXYGENS	
Si	0.000	0.000	0.000	4.038	4.068
				4.038	4.068
Al	0.035	0.016	0.025	0.015	0.010
Ti	0.000	0.000	0.000	0.002	0.003
Fe	0.472	0.388	0.181	0.146	0.265
Mg	0.043	0.077	0.085	0.159	0.035
Ca	0.000	0.004	0.004	0.006	0.006
Mn	0.000	0.000	0.000	0.012	0.013
Sn	0.023	0.011	0.008	0.004	0.004
Cu	0.158	0.171	0.213	0.086	0.117
Ni	8.987	9.250	9.463	7.118	6.850
Zn	0.241	0.063	0.000	0.363	0.550
	9.559	9.980	9.979	7.511	7.853

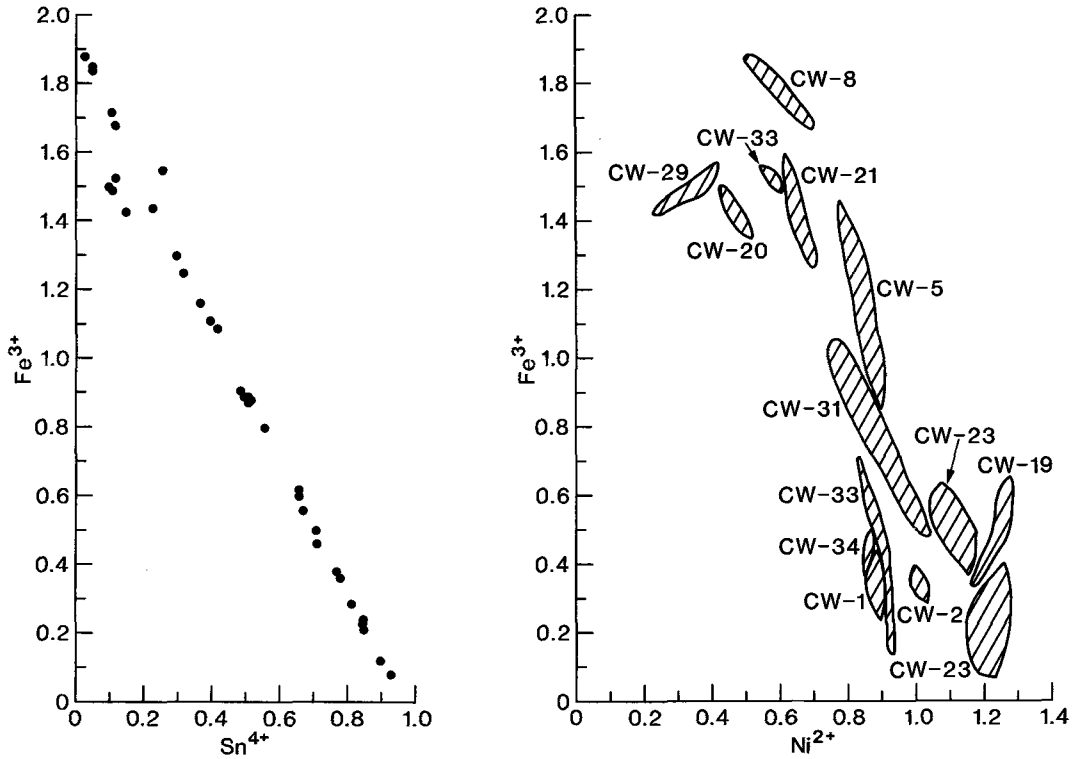

FIGS. 3 and 4. FIG. 3 (*left*). Plot of Fe^{3+} against Sn^{4+} for opaque spinels from CW-23, 31, 5, 29, and 8 (cations per 4 oxygens). FIG. 4 (*right*). Plot of Fe^{3+} against Ni^{2+} for opaque spinels (cations per 4 oxygens).

ions in the *Y* (octahedrally co-ordinated) sites. Therefore, the excess divalent cations are equal to the amount of Sn^{4+} in the *Y* sites, due to the replacement $2Fe^{3+} \rightleftharpoons Sn^{4+} + R^{2+}$. This $Fe^{3+} \rightleftharpoons Sn^{4+}$ substitution in the spinels is illustrated by fig. 3.

Ni^{2+}/Zn^{2+}-Fe^{3+}. The cations Fe^{3+} and Zn^{2+} vary independently of each other. In comparison the plot Fe^{3+}-Ni^{2+} (fig. 4) defines an apparent $Ni^{2+} \rightleftharpoons Fe^{3+}$ substitution. This is probably because Ni^{2+} enters the spinel to charge-balance Sn^{4+} and, therefore, can act in the same way as Fe^{2+} does between magnetite and ulvöspinel. Cation proportions show that in the most tin-rich spinels, Ni^{2+} cannot account for all the Sn^{4+}. This may be due to either the availability of Ni^{2+} or the solubility limit for $Ni_2^{2+}Sn^{4+}O_4$ in spinel. Analysis CW23F (Table II) gives an upper limit of 64% Ni_2SnO_4 molecule (assuming all Ni^{2+} to be in this hypothetical molecule).

Chemical variation amongst the divalent cations has been investigated by plotting them against each other. The resultant relationships will be described, although only the most important will be reproduced graphically.

Ni^{2+}-Zn^{2+} (fig. 5). The concentration of Ni^{2+} appears to be independent of Zn^{2+}. The spinels of assemblage 2 (Table II) have more than 0.8 cations (per 4 oxygens) of Ni^{2+}; the Zn^{2+} content varies between 0.06 and 0.73 cations depending on the sample. Those from assemblage 3 have less than 0.7 cations of Ni^{2+} (except CW-4) and less than 0.2 cations of Zn^{2+}.

Ni^{2+}/Zn^{2+}-Fe^{2+} (fig. 6). In most samples the Fe^{2+} has a limited compositional range, with an upper limit of 0.50 cations (CW-29). The concentration of Fe^{2+} is generally independent of Ni^{2+} and Zn^{2+}; the plot of Ni^{2+}-Fe^{2+} is reproduced in fig. 6. However, samples CW-8, 20, and 29 do suggest some $Ni^{2+} \rightleftharpoons Fe^{2+}$.

$Ni^{2+}/Zn^{2+}/Fe^{2+}$-Cu^{2+}. In general, Cu^{2+} is independent of the other divalent cations.

Consequently, the relations between the end-members are complex but the phase can be described as ranging between a $(Ni,Fe^{2+})Fe_2^{3+}O_4$-rich spinel and a Ni_2SnO_4-rich spinel.

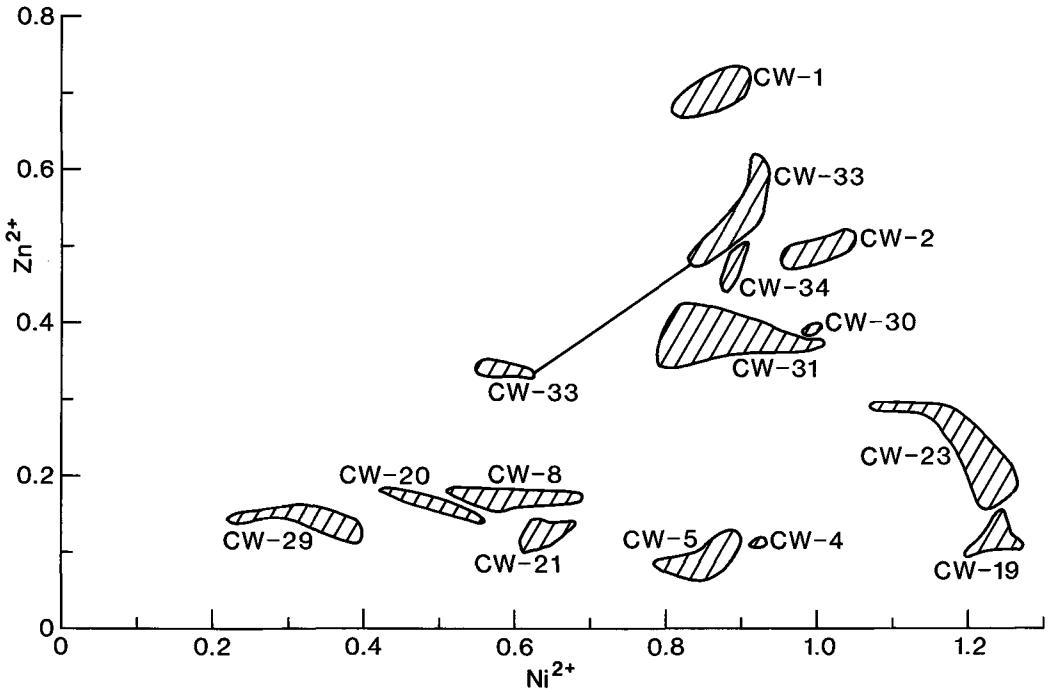

FIG. 5. Plot of Zn^{2+} against Ni^{2+} for opaque spinels (cations per 4 oxygens).

Delafossite

A plot of $2Fe^{3+}$ against $Ni^{2+}+Sn^{4+}$ (fig. 7) shows that Sn^{4+} is able to substitute for Fe^{3+}, as in spinels, with Ni^{2+} entering to balance the charges.

Cu content of the mineral phases

The dissolved Cu crystallizes as delafossite and cuprite, and also enters the structure of nickel-olivine (up to 1.12 wt. % CuO), bunsenite (up to 2.26 wt. % CuO), and spinel (up to 2.96 wt. % CuO). These relative values suggest that CuO is most soluble in the spinel.

Cu^{2+} in the spinels is generally independent of the other divalent cations, although the highest values coincide with delafossite-bearing samples. There is no evidence to support the idea of Altman *et al.* (1976) that the CuO content of spinel is temperature-dependent, although this would explain the apparent variation in CuO content for crystals in the same sample.

Ni and Sn contents of the mineral phases

The three recognized mineral assemblages are essentially the same, since *assemblage 1* = *assemblage 3* + $NiO + SnO_2$ and *assemblage 2* = *assemblage 3* + SnO_2. This dominance by spinel, delafossite, and cuprite (i.e. assemblage 3) can be attributed to (i) the large proportion of CuO_2 in the bulk chemical compositions, and (ii) the low preference for the other oxides (except NiO) to combine with SiO_2 to crystallize a silicate mineral.

Tin is normally incompatible during the crystallization of spinels; however, Sn^{4+} becomes very compatible when spinel crystallizes in association with cassiterite (Wearing, 1983). Consequently, the spinels of assemblage 2 (and assemblage 1) are SnO_2-rich, as are the associated delafossites.

The chemical data suggest that nickel plays the role of the charge-balancing divalent cation when Sn^{4+} enters the octahedral sites of spinel and delafossite. The relative amounts of NiO, ZnO, and FeO in the spinel are related to their concentrations in the liquid (Wearing, 1981), although Ni^{2+} is known to have greater crystal-field stabilization energy in octahedral co-ordination than in tetrahedral co-ordination.

Overall, the bulk chemical compositions appear to control the mineral chemistry, in particular causing the complex nickel- and tin-rich character of the spinel and delafossite phases.

Acknowledgements. The samples were provided by I.M.I. Refiners Limited, and the author gratefully acknowledges

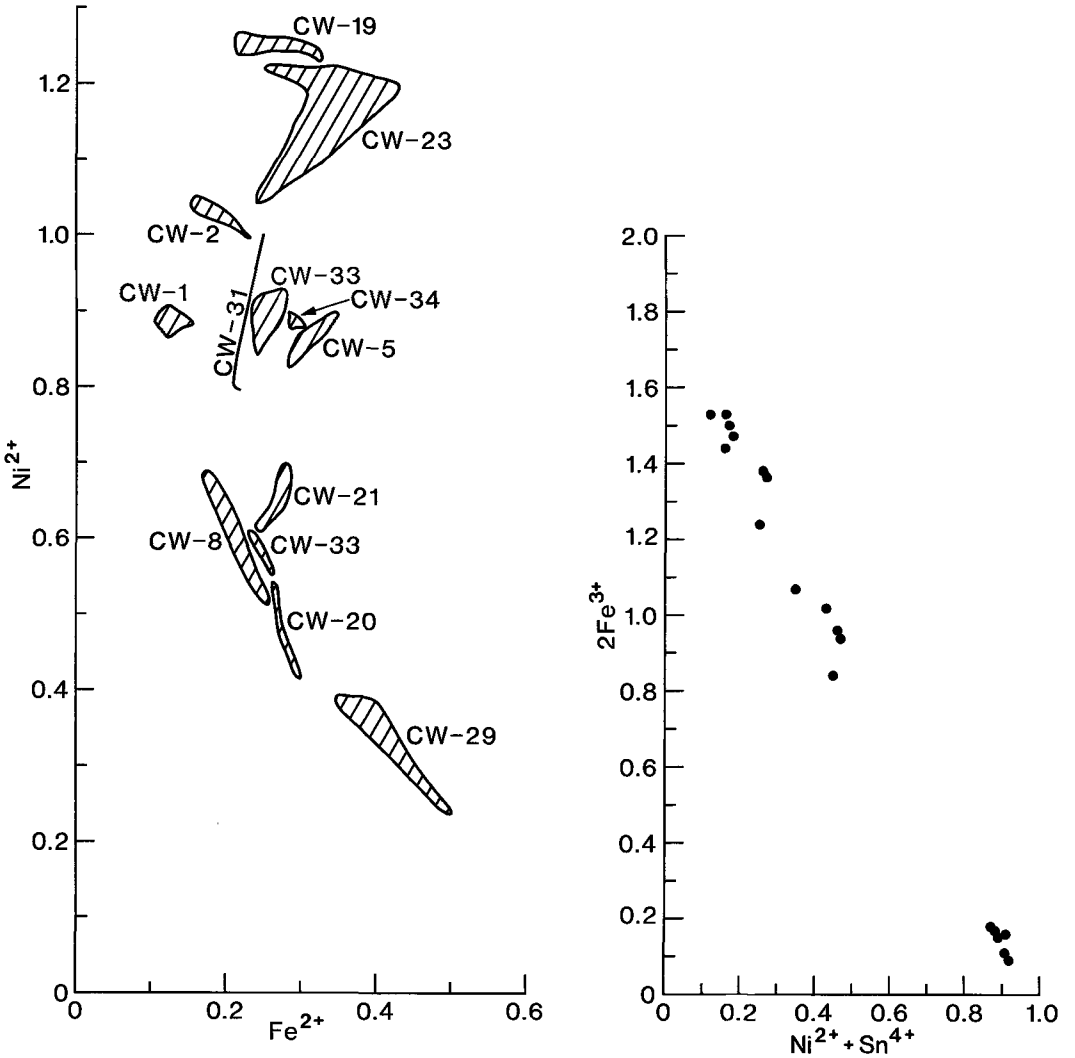

FIGS. 6 and 7. FIG. 6 (*left*). Plot of Ni^{2+} against Fe^{2+} for opaque spinels (cations per 4 oxygens). FIG. 7 (*right*). Plot of $2Fe^{3+}$ against $Ni^{2+} + Sn^{4+}$ for delafossite (cations per 2 oxygens).

their permission to publish this paper. The technical assistance of Dr N. Charnley, Messrs S. M. Baker, C. R. Fagg, P. J. Jackson, R. McAvoy, K. A. Parrish, M. Slater, and the late R. A. Holland is particularly acknowledged. This work was supported by the NERC and supervised by Dr. B. C. M. Butler.

REFERENCES

Altman, R., Schlein, W., and Silva, C. (1976) *Extractive Metallurgy of Copper, International Symposium*, **1** (Yannopoulos, J. C., and Agarwal, J. C., eds.), 296–316.

Butler, B. C. M. (1978) *Mineral. Mag.* **42,** 487–92.

Edwards, A. B. (1949) *Proc. Australas. Inst. Mining Metall.* **154–5,** 41–67.

Ott, W. R., and McLaren, M. G. (1970) *J. Am. Ceram. Soc.* **53,** 374–5.

Wearing, E. (1981) Unpub. D.Phil. thesis, Univ. of Oxford.

——(1983) *Mineral. Mag.* **47,** 335–45.

[*Manuscript received 1 February 1983; Revised 2 September 1983*]